

Designing Hybrid Antibiotic Peptide Conjugates To Cross Bacterial Membranes

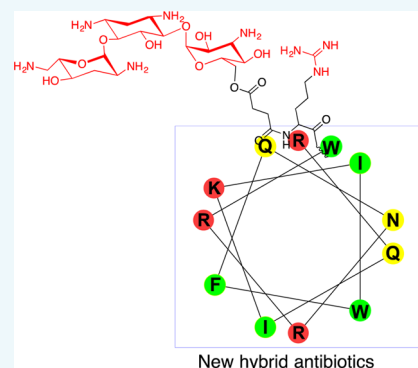
Stephanie Deshayes,[†] Wujing Xian,[†] Nathan W. Schmidt,[‡] Shadi Kordbacheh,[†] Juelline Lieng,[†] Jennifer Wang,[†] Sandra Zарner,[†] Samantha St. Germain,[†] Laura Voyer,[†] Julia Thulin,[†] Gerard C. L. Wong,^{*,†,‡,§} and Andrea M. Kasko^{*,†,§}

[†]Bioengineering Department, [‡]Chemistry and Biochemistry Department, and [§]California NanoSystems Institute, University of California, Los Angeles, 410 Westwood Plaza, Los Angeles, California 90095-1600, United States

[‡]Department of Pharmaceutical Chemistry, University of California, San Francisco, 555 Mission Bay Boulevard South, San Francisco, California 94158, United States

S Supporting Information

ABSTRACT: We design hybrid antibiotic peptide conjugates that can permeate membranes. Integration of multiple components with different functions into a single molecule is often problematic, due to competing chemical requirements for different functions and to mutual interference. By examining the structure of antimicrobial peptides (AMPs), we show that it is possible to design and synthesize membrane active antibiotic peptide conjugates (MAAPCs) that synergistically combine multiple forms of antimicrobial activity, resulting in unusually strong activity against persistent bacterial strains.



INTRODUCTION

Aminoglycosides are a clinically important class of antibiotics. The first aminoglycoside streptomycin was isolated from the actinobacterium *Streptomyces griseus* in 1943 and was the first medicine effective against tuberculosis infections. Since then, over 150 naturally occurring aminoglycosides have been isolated either from *Streptomyces* genus or *Micromonospora* bacteria. They have been mostly used for the treatment of serious infections caused by aerobic Gram-negative bacteria, but also exhibit moderate potency against Gram-positive pathogens.¹ Aminoglycosides are bactericidal agents that block protein synthesis by binding to the 30S subunit of the bacterial ribosome.^{2–4} The most therapeutically relevant aminoglycoside antibiotics are gentamicin, tobramycin, amikacin, kanamycin, and neomycin.

Although aminoglycosides are highly potent antibiotics, bacterial resistance to this class has drastically increased.^{3,5,6} The main mechanisms of aminoglycoside resistance are (i) a reduced uptake/drug efflux; (ii) enzymatic inactivation of the aminoglycoside through adenylation, acetylation, or phosphorylation; and (iii) target modification such as ribosomal methylation and mutations.^{3,6} While several approaches have been used to generally address aminoglycoside resistance, a particular research effort has focused on counteracting enzymatic inactivation. For example, one of the strategies is the development of competitive inhibitors of aminoglycoside-modifying enzymes.^{7–9} However, none of these inhibitors

appear to be especially effective, and they may inhibit host proteins and cause side effects. Chemical modification of aminoglycosides that renders them less susceptible to enzymatic inactivation has been another widely reported approach to combat bacterial resistance.^{10–13} While numerous aminoglycoside analogs have been developed, very few have reached clinical trials since the 1990s. Recently, Plazomicin, a semisynthetic aminoglycoside derived from sisomicin, has been developed by Achaogen Inc. and is in Phase III clinical trials. Plazomicin demonstrated good activity against Gram-negative and Gram-positive bacteria but is not active against bacterial isolates expressing ribosomal methyltransferases conferring aminoglycoside resistance.^{14,15}

Increasing the influx of antibiotics through the bacterial membrane barrier may be an alternative strategy to increase the activity of antibiotics against resistant strains of bacteria. In the past few decades, our understanding of the mechanisms of drug uptake and drug extrusion has advanced substantially.¹⁶ The balance between the influx and efflux processes ultimately determines the amount of drug accumulated in bacterial cells. Efflux pumps are found in almost all bacterial species, and a

Special Issue: Peptide Conjugates for Biological Applications

Received: December 19, 2016

Revised: February 6, 2017

Published: March 1, 2017

strong correlation of efflux system overexpression with multidrug resistance has been demonstrated.¹⁶ Efflux systems actively pump antibiotics out to reduce cellular drug accumulation, thus facilitating bacterial survival. This effect also contributes to the formation of drug-tolerant persister cells.¹⁷ Reduced antibiotic concentration inside a target cell by activation of drug efflux not only affects the susceptibility of the strain to the antibiotic but also drives the acquisition of additional resistance mechanisms.

In Gram-negative bacteria, an important factor that influences antibiotic concentration is membrane permeability.¹⁸ The outer membrane (OM) of Gram-negative bacteria serves as a remarkable barrier and provides an extra layer of defense against toxic compounds. Small hydrophilic molecules such as β -lactams passively and rapidly cross the OM through porins (water-filled open channels) while hydrophobic drugs gain access to the cell interior by a slow metabolic activity-dependent mechanism.¹⁸ Reduced permeability, which has been observed in various multidrug resistant strains,^{18,19} may occur via a variety of mechanisms, such as a loss or modification of porins or an alteration of the phospholipid composition of the outer leaflet. Diminished permeability is also responsible for the reduced accumulation of antibiotic in persister cells. Positively charged antibiotics such as aminoglycosides do not diffuse through bacterial membranes well (compared to neutral, hydrophobic drugs), due in part to the large electrostatic self-energy of such molecules in low dielectric constant media such as lipids. Although the exact mechanism of aminoglycoside uptake remains unclear, it has been proposed to occur through an active-transport mechanism that is energy dependent and relies on the generation of proton-motive force (PMF).^{20,21} Compared to diffusive transport, this mechanism is slow. Moreover, PMF can be shut down in persister cells, and thereby impact the influx of aminoglycosides.²⁰ As a result, efflux pumps can easily counteract the slow drug influx of aminoglycosides. These various mechanisms that decrease drug uptake explain why aminoglycosides are not active against a wide variety of microbes, including anaerobic bacteria and persister cells.^{20–24}

Antimicrobial peptides (AMPs), powerful effectors of innate immunity, have been considered as a possible treatment for resistant bacteria. AMPs have broad spectrum antimicrobial activity^{25–28} and utilize nonspecific interactions to target generic features common to the outer membranes of many pathogens, hence development of resistance to such natural defenses is inhibited compared to conventional antibiotics.²⁵ Hydrophobicity and cationic charge are both known to be necessary conditions for antimicrobial activity in a broad range of AMPs. In previous work, we found that the membrane permeation activity of a wide range of AMPs is correlated with the induction of negative Gaussian curvature in model bacterial membranes, which topologically enables membrane destabilizing processes²⁹ such as pore formation, blebbing, and budding.³⁰ The main limitation of using AMPs as antibiotics is their moderate potency.³¹

Conferring membrane permeability to aminoglycosides should increase their uptake in bacteria. Furthermore, efflux pumps are not effective for higher molecular weight drugs, and thus, increasing the molar mass of aminoglycosides may promote their accumulation in bacteria. In order to simultaneously increase the membrane permeability of aminoglycosides and increase their molar mass, we engineered a membrane-active antibiotic–peptide conjugate (MAAPC),

Pentobra, which conjugates a short peptide transporter sequence derived from penetratin, a cell-penetrating peptide, with the aminoglycoside tobramycin. Pentobra kills bacteria in distinct mutually amplifying ways by simultaneously targeting different bacterial functions (membrane integrity and protein synthesis). This combination also promotes rapid drug entry into persistent cells via AMP-like membrane permeation. The mistranslated proteins from aminoglycoside activity further stress the membrane barrier function. Pentobra exhibits potent and broad-spectrum antimicrobial activity against bacteria that are not susceptible to aminoglycosides such as persistent cells²⁴ and anaerobic *Propionibacterium acnes*.³²

In this report, we engineer a series of membrane-active antibiotic–peptide conjugates (MAAPCs) using our design principles for selective bacterial membrane permeation. Specifically, we examine how variations in the peptide transporter sequence from MAAPC01, Pentobra, modulate antibacterial activity and membrane permeation abilities. This series of MAAPCs, collectively, tests the effects of peptide sequence, average hydrophobicity, helical amphiphilicity, peptide–tobramycin conjugation site and linker chemistry, properties that are considered important for the antimicrobial profiles of AMPs and conjugate antibiotics. Distinct and synergistic mechanisms of killing are incorporated into a unimolecular drug in order to create multilethal, broad-spectrum antibiotics with activity against antibiotic-resistant strains. The result is a versatile platform of novel multilethal MAAPCs based on deterministic design principles.

RESULTS AND DISCUSSION

MAAPC Synthesis. Combining the membrane activity of AMPs with traditional antibiotics allows the delivery of antibiotics that have been historically difficult to get across bacterial membranes. MAAPCs comprise a potent antibiotic (i.e., tobramycin) and a peptide transporter sequence that enables membrane permeation. It is helpful to consider the mechanism of membrane activity in molecules such as AMPs when designing these hybrid antibiotics, because simply linking two molecules together can lower the activity of both of them by functional interference. Without a specific guidance methodology it is difficult to design chemically and structurally diverse compounds with consistently robust antimicrobial profiles. We recently identified sequence principles for peptides that permeate membranes based on induced curvature considerations.^{28,29,33–36} We have demonstrated that the geometric need to generate negative Gaussian curvature places constraints on the amino acid sequence in AMPs.³³ In fact, a recent machine learning study suggests that the probability a given amino acid sequence is antimicrobial is related to its ability to induce negative Gaussian curvature.³⁷ The lysine/arginine ratio increases sharply with the hydrophobic content of an AMP, a trend that can be observed in the sequences of 1080 cationic AMPs.³⁵ Importantly, because membrane disruption depends on the arginine, lysine, and hydrophobic residue content in AMPs, the sequence constraints for membrane activity under-determine the full sequence, so that it is possible to blend different functions into the same sequence. For this reason, it is possible to impart molecules like polycationic aminoglycosides with membrane activity.

In order to compare the effect of the peptide transporter sequence on membrane permeabilization and biological activity, we renovated a single aminoglycoside antibiotic, tobramycin. We chose tobramycin because it is a standard-of-care for many

types of *Pseudomonas aeruginosa* infections including pulmonary infections in patients with cystic fibrosis.³⁸ In addition, the sole primary hydroxyl group in tobramycin is amenable to selective conjugation. Indeed, the primary hydroxyl group of tobramycin is a more effective nucleophile and less hindered than its secondary hydroxyl groups, which facilitates its modification, as it does not require orthogonal protection of the secondary hydroxyl groups. Furthermore, this primary hydroxyl group does not participate in specific interactions with the ribosome, such that the biological activity of the modified tobramycin should not be impacted by the conjugation.^{39,40}

The peptide transporter sequences of the MAAPCs listed in Table 1 are based on sequence motifs found within natural

Table 1. New MAAPCs Based on Induced Curvature Considerations

MAAPC	other name	peptide sequence	N- or C-terminal conjugation
	penetratin	RQIKIWFQNRRMKWKK	
MAAPC01	Pentobra	RQIKIWFQNRRW	N-terminal
MAAPC02		GWIRNQFRKIWQR	N-terminal
MAAPC03		GWRRNQFWIKIQR	N-terminal
MAAPC04		GWRNQIRKQGWQR	N-terminal
MAAPC05		RQIKIWFQNRRW	C-terminal

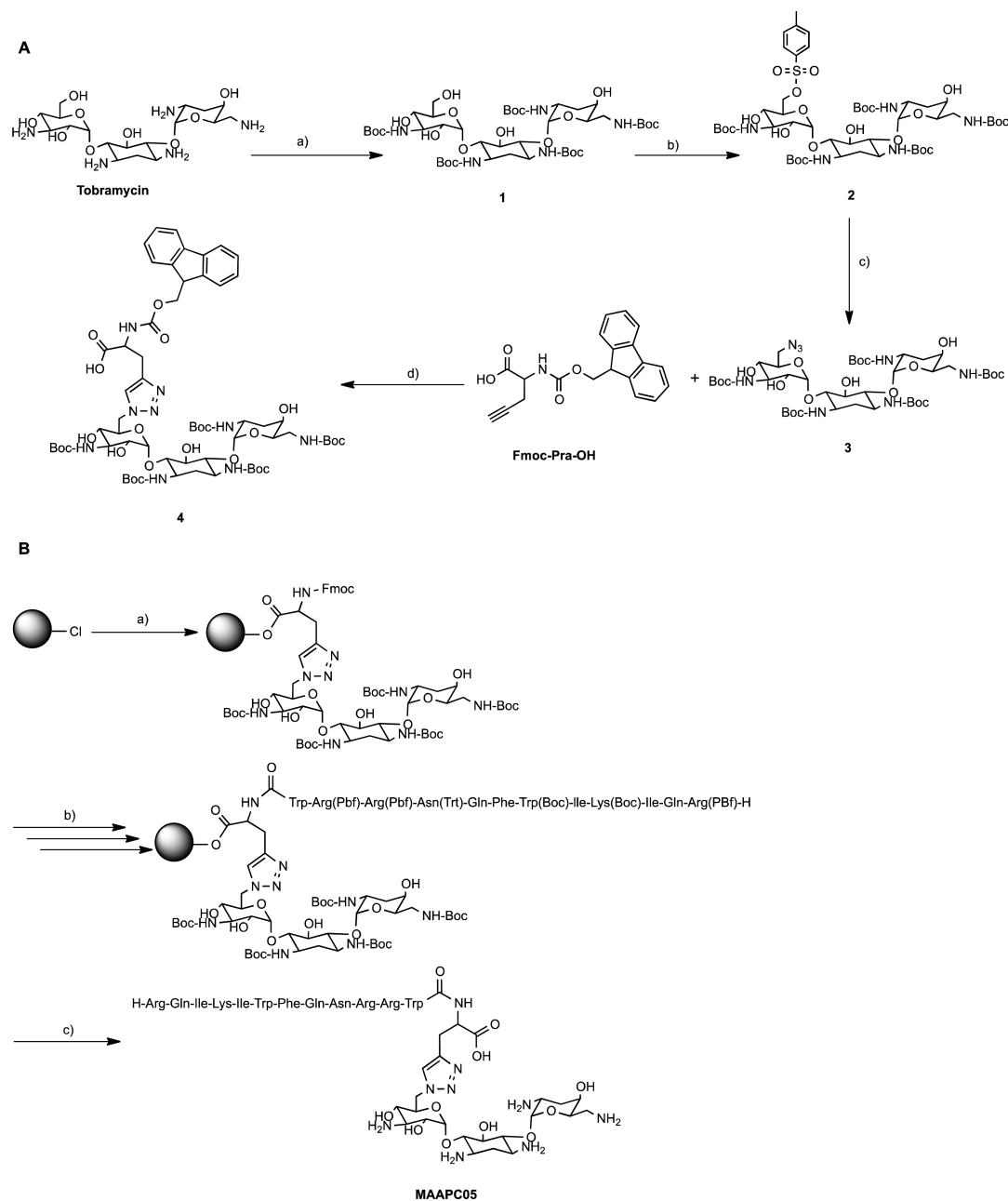
AMPs (and specifically penetratin) and our saddle-splay curvature selection rules. By changing the peptide hydrophobicity and the number of cationic charges, we effectively tune the degree to which the drug will associate with the bacterial membrane. A good balance between hydrophobic and cationic groups is crucial to achieving selective bacterial membrane disruption.

MAAPC02, MAAPC03, and MAAPC04 were synthesized employing a procedure similar to Pentobra (also identified in this manuscript as MAAPC01) in which tobramycin is attached to the N-terminus of the peptide through a short linker by amide bond (Figure S1).²⁴ MAAPC05 has the same peptide sequence as MAAPC01, but tobramycin is conjugated to the C-terminus through a synthetic amino acid, L-propargylglycine, via “click” chemistry (Scheme 1). Thus, tobramycin is connected through a stable 1,2,3-triazole ring, which is less susceptible to hydrolysis than an ester bond found in MAAPC01. In order to achieve the “click” coupling with a terminal alkyne, tobramycin was functionalized with an azide group using an adapted literature protocol.⁴¹ Briefly, after protection of the amine groups of tobramycin as *tert*-butoxycarbamates (Boc) (compound 1), the primary hydroxyl at the C6'' position was activated with *p*-toluenesulfonyl chloride (TsCl) in pyridine giving the monotosylated compound 2, which was subsequently substituted with an azide function using sodium azide (NaN₃) in DMF at 80 °C producing azido-Boc₅-tobramycin 3 (Scheme 1A). The azido-modified tobramycin (3) was then “clicked” with Fmoc-protected L-propargylglycine (Fmoc-Pra-OH) via copper(I)-catalyzed azide–alkyne 1,3-dipolar cycloaddition reaction affording Fmoc-Pra(BocTobra)-OH (4) (Scheme 1A). Compound 4 was grafted to the 2-chlorotrityl chloride resin as the first residue of the peptide sequence (Scheme 1B). The peptide synthesis was then carried out following standard Fmoc strategy. Finally, the peptide was cleaved from the resin and fully deprotected using a mixture of trifluoroacetic acid (TFA) and scavengers to yield MAAPC05 (Scheme 1B).

MAAPC Structures: Similarities and Differences. The MAAPC peptide designs are based on penetratin, a cell-penetrating peptide (CPP) isolated from the homeobox domain of the ANTP protein. CPPs, like AMPs, interact strongly with membranes and are cationic and amphiphilic. There is no strict distinction between the two peptide classes, although CPPs are generally less hydrophobic than AMPs.²⁹ Many AMPs have been shown to cross bacterial membranes in the CPP-like manner and exert antimicrobial activity by binding intracellular targets, and certain CPPs are antibacterial *in vitro*.²⁸ All MAAPCs in this report contain tobramycin, which binds to the tRNA decoding A-site in prokaryote ribosomes.^{2–4}

The first MAAPC, Pentobra (MAAPC01) and the other peptide sequences were selected in concert with the physicochemical properties of tobramycin such that the conjugate possesses a specific total cationic charge that favors membrane penetration and permeabilization in bacteria. The new MAAPCs share many similarities in sequence and amino acid composition (Tables 1 and 2), but were designed to differ in important ways, in order to examine how specific peptide characteristics affect the ability of MAAPCs to target bacteria and optimize activity. We focused on the effects of peptide sequence, hydrophobicity, helix amphiphilicity, the linker used to connect the peptide with tobramycin, and N-terminal vs C-terminal conjugation. Penetratin comprises 16 amino acids, whereas all of the transporter sequences are shorter, with 12 or 13 amino acids (Table 2). Penetratin and each of the transporter sequences each possess the same number of arginine, glutamine, asparagine, and tryptophan residues (Table 2). The net charge of penetratin is +7, whereas the peptide–tobramycin conjugates have a net charge of +9.

Figure 1 depicts the helical wheel projections of the MAAPCs in comparison to penetratin. It is important to note that (a) rotational freedom along σ bonds means the tobramycin may not sit exactly where depicted in this figure and (b) the size of the helical wheel is not depicted to the scale of the aminoglycoside. Despite these limitations, Figure 1 does allow us to compare structures of the MAAPCs to penetratin. Penetratin has a cluster of mostly cationic residues (RKKQR) flanked by multiple hydrophobic residues on either side (FWIRW and MI). MAAPC01 shows the greatest clustering of cationic character when the cationicity of tobramycin is included in addition to the cationic residues (RKQR-tobramycin). The amino acid composition MAAPC02 differs from MAAPC01 by the addition of a single glycine at the N-terminus, and the residues in MAAPC02 are rearranged to create a sequence in which the cationic and hydrophobic residues cluster on opposing sides of the peptide helical wheel diagram (Figure 1). This type of amphiphilicity is observed in α -helical AMPs sequences, and is often important for antibacterial activity.⁴² MAAPC03 has the reverse sequence of MAAPC01, and has identical amino acid composition to MAAPC02 but the amino acid residues are in a different sequence to exhibit greater amphipathicity. A reverse peptide sequence, in principle, is expected to have equivalent antibacterial activity as the original if activity is derived solely from nonspecific interactions with bacterial membranes. Helical amphiphilicity is also present in MAAPC04, but the hydrophobic content of the peptide is reduced from 38.5% to 25% (Table 3) by removing one isoleucine and the phenylalanine and replacing these bulky hydrophobic residues with glycines (Table 2). A comparison of MAAPC04 with the more hydrophobic MAAPC01 allows us to investigate the effects of

Scheme 1. Synthesis of MAAPC05^a

^a(A) Synthesis of Fmoc-Pra(BocTobra)-OH (4): (a) Boc_2O , TEA, $\text{H}_2\text{O}/\text{DMF}$ (1:4), 5 h, 60 °C, 93%;²⁴ (b) TsCl, pyridine, 12 h, 23 °C, 36%; (c) NaN_3 , DMF, 12 h, 80 °C, 99%; (d) CuSO_4 , sodium ascorbate, DMF, 24 h, 40 °C, 61%. (B) Grafting of Fmoc-Pra(BocTobra)-OH to 2-chlorotrityl chloride resin ((a) compound 4, DIEA, DCM, 4 h, 23 °C followed by peptide synthesis on solid support using Fmoc strategy ((b) Fmoc cleavage using piperidine and coupling using DIEA, HOBt, and HBTU), and final cleavage and deprotection of the peptide using a mixture of trifluoroacetic acid (TFA) and scavengers ((c) TFA/phenol/water/thioanisole/TIS (10:0.7:0.5:0.5:0.25 v/w/v/v/v), 3 h, 23 °C, 46%). The gray sphere represents the 2-chlorotrityl chloride resin.

Table 2. Composition of Peptide Transporter Sequences

	R	Q	K	N	W	I	F	G	M	net charge
Penetratin	3	2	4	1	2	2	1	0	1	+7
MAAPC 01/05	3	2	1	1	2	2	1	0	0	+9
MAAPC 02/03	3	2	1	1	2	2	1	1	0	+9
MAAPC4	3	2	1	1	2	1	0	2	0	+9

reducing peptide hydrophobicity on membrane permeation and antibacterial activity. To explore the additional degree of freedom afforded by conjugation chemistry we connected tobramycin to the C-terminus of the Pen peptide from MAAPC01. The resulting MAAPC05 has a different chemical structure in the linker that is proximal to tobramycin.

The arrangement of a cationic patch flanked by hydrophobic residues (as seen in penetratin) is best replicated by MAAPC01, where the aminoglycoside is located near the cluster of cationic residues. MAAPC05 also colocalizes the

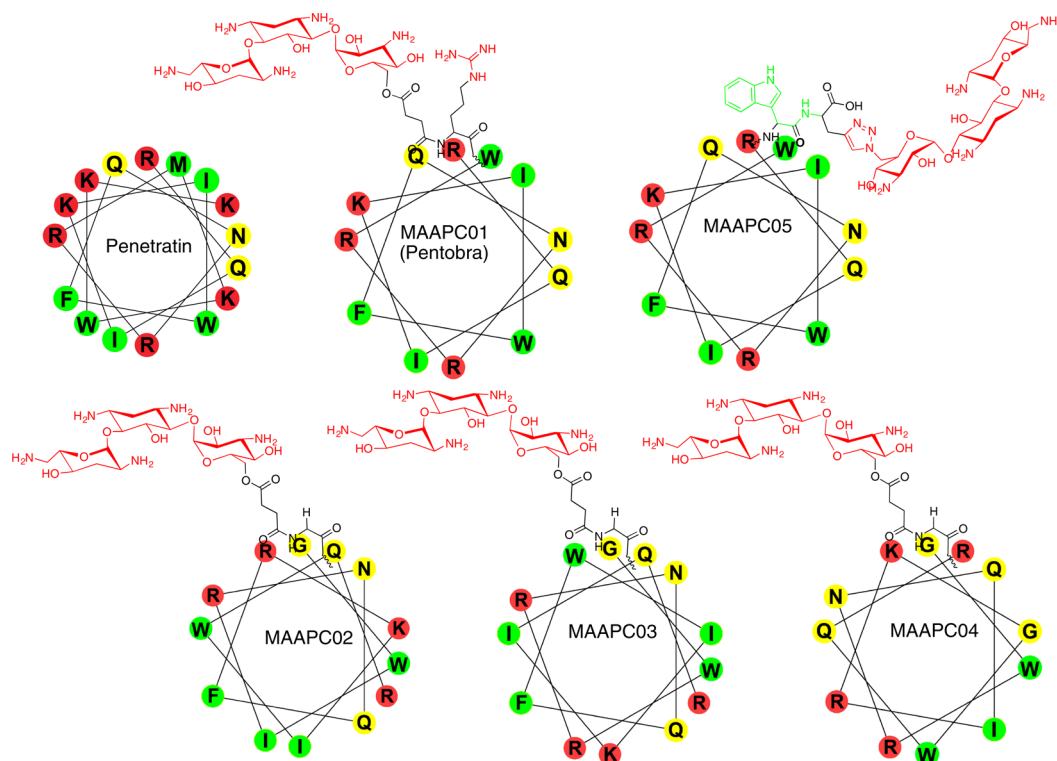


Figure 1. Helical wheel projections of MAAPCs. Cationic residues are represented in red, hydrophobic residues are represented in green, and neutral amino acids are in yellow.

Table 3. Hydrophobicity of Peptide Transporter Sequences^a

	% hydrophobic	Eisenberg consensus	Kyte Doolittle (GRAVY)	Wimley-White	N_K/N_R	$N_{\text{primary amines}}/N_R$
Penetratin	37.5	-0.54	-1.73	-1.50	0.75	0.75
MAAPC01/05	41.7	-0.47	-1.49	-1.36	0.33	2
MAAPC02/03	38.5	-0.42	-1.41	-1.31	0.33	2
MAAPC04	25	-0.55	-2.17	-1.55	0.33	2

^a N_K and N_R are the numbers of lysine and arginine residues respectively. $N_{\text{primary amines}}$ refers to the number of primary amines (from lysine and tobramycin).

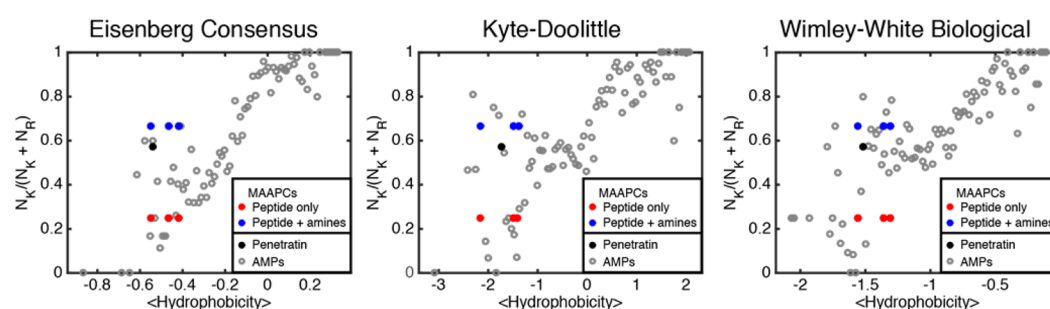


Figure 2. Cationic behavior of MAAPCs, plotted as the ratio of the number of amines in each molecule to its total cationic charge, as a function of average peptide hydrophobicity calculated with Eisenberg Consensus,⁴³ Kyte-Doolittle,⁴⁴ and Wimley-White⁴⁵ amino acid hydrophobicity scales. AMPs are represented by unfilled gray circles, MAAPC peptides by red circles, MAAPCs plus the charge contribution of the five amine groups in tobramycin by blue circles, and the black circle represents penetratin CPP.

aminoglycoside with the cationic residues, but the overlap is not as great since attachment to the tryptophan residue orients it away from the cationic face. In this instance, however, rotation about the N–C bond of the tryptophan carbon would bring the aminoglycoside closer to the cationic face. MAAPC02 has a hydrophobic face and a cationic face, but the cationic face has neutral residues on one site, in contrast to penetratin. MAAPC03 is similar to MAAPC05; however, the rigidity of

the peptide bond will direct the aminoglycoside chain such that it cannot sit directly over the neutral residues. Finally, MAAPC04 has a large cationic side, and only a small patch of hydrophobic residues.

MAAPC01 and 05 have the highest percentage of hydrophobic residues at 41.7% (Table 3); MAAPC02 and 03 are comparable to Penetratin (38.5% and 37.5%, respectively), while MAAPC04 has the lowest number of hydrophobic

Table 4. MIC and MBC of MAAPCs, Unconjugated Peptides (P1–P4), Mixture of Unconjugated Peptide and Tobramycin (P1–P4+Tobramycin), and Tobramycin Alone on *E. coli* MG1655 and *S. aureus* S113^a

	<i>E. coli</i> MG1655		<i>S. aureus</i> S113	
	MIC (μM)	MBC (μM)	MIC (μM)	MBC (μM)
MAAPC01	6.3 \pm 0.0	6.3 \pm 0.0	25.0 \pm 0.0	33.3 \pm 14.4
MAAPC02	3.1 \pm 0.0	3.1 \pm 0.0	12.5 \pm 0.0	20.8 \pm 7.2
MAAPC03	<1.6	3.1 \pm 0.0	12.5 \pm 0.0	25.0 \pm 0.0
MAAPC04	3.1 \pm 0.0	4.2 \pm 1.8	12.5 \pm 0.0	14.6 \pm 9.5
MAAPC05	12.5 \pm 0.0	12.5 \pm 0.0	25.0 \pm 0.0	25.0 \pm 0.0
P1	12.5 \pm 0.0	12.5 \pm 0.0	50.0 \pm 0.0	50.0 \pm 0.0
P2	41.7 \pm 14.4	41.7 \pm 14.4	33.3 \pm 14.4	>100
P3	16.7 \pm 7.2	16.7 \pm 7.2	100.0 \pm 0.0	>100
P4	>100	>100	100.0 \pm 0.0	>100
P1+tobramycin	<1.6	3.1 \pm 0.0	3.1 \pm 0.0	5.2 \pm 1.8
P2+tobramycin	<1.6	2.1 \pm 0.9	6.3 \pm 0.0	12.5 \pm 0.0
P3+tobramycin	2.1 \pm 0.9	2.6 \pm 0.9	6.3 \pm 0.0	12.5 \pm 0.0
P4+tobramycin	<1.6	3.6 \pm 2.4	3.1 \pm 0.0	6.3 \pm 0.0
Tobramycin	<1.6	3.1 \pm 0.0	6.3 \pm 0.0	6.3 \pm 0.0

^aNotes: P1–P4 are the peptides in MAAPC01–04, respectively. MAAPC05 has the same peptide sequence as MAAPC01 and can be directly compared to P1. MIC/MBC values are expressed in μM for a fair comparison of tobramycin activity either as an antibiotic alone or as a conjugate. Values are mean \pm standard deviation of a sample analyzed in triplicate.

residues (25%). The hydrophobicity of the MAAPCs in comparison to penetratin and other AMPs can also be observed in plots of the ratio of lysines to total cationic charge versus average molecule hydrophobicity (Figure 2). The peptide “transporter” sequences clearly lie along the AMP sequence trendline (Figure 2), with the MAAPCs 01 and 05 having the greatest average hydrophobicity, followed by MAAPCs 02 and 03, and finally MAAPC04. Their positions demonstrate that all MAAPC peptides except MAAPC04 are more hydrophobic and arginine-rich than the parent penetratin peptide. Moreover, penetratin is less hydrophobic than AMPs with comparable lysine/cationic charge ratio, which is consistent with its classification as a CPP. If we account for the presence of tobramycin in the MAAPCs by considering its entire contribution to be charged from the five amine groups, then the molecules are located closer to penetratin on the plot and are expected to behave more like cell-penetrating peptides. This simple characterization of the physicochemical properties of tobramycin does not account for pK_a differences in the amino groups and the influence of other chemical moieties in tobramycin, however, and the actual locations of the MAAPCs are likely to be between the peptide only and peptide + amine positions. The MAAPCs are therefore expected to possess membrane permeabilization and drug transporter abilities, the desired attributes of multifunctional antibiotics that act on both bacterial membranes and ribosomes. Together, these five MAAPCs provide insight into the effects that sequence, hydrophobicity, amphiphilicity, and linker chemistry have on antibacterial activity.

Activity Spectrum. We first investigated the antimicrobial potency of these new MAAPCs by determining their minimum inhibitory concentration (MIC) and minimum bactericidal concentration (MBC) against *Escherichia coli* (*E. coli* MG1655) and *Staphylococcus aureus* (SA113) pathogens with a turbidity-based microdilution broth assay (Table 4). Overall, all the MAAPCs display good antimicrobial activity and tend to be more selective to *E. coli* (MIC range 3.1–12.5 μM) over *S. aureus* (MIC range 12.5–25 μM), which follows the general observation that tobramycin is particularly active against Gram-negative organisms.⁴⁶ Their MBC values are either equal to or

slightly higher than their respective MIC values suggesting that the compounds not only are inhibiting bacterial growth but are also bactericidal. In contrast, the unconjugated peptides (P1–P4) exhibited no or little antimicrobial activity against *E. coli* and *S. aureus*. However, the MAAPCs did not show better activity than tobramycin, which is expected because our conjugates are not designed to target lab strains but instead to have high efficacy against clinically relevant pathogens such as persisters, resistant bacteria, and anaerobes that are impermeable to existing antibiotics. It should be noted that a mixture of the peptide itself with tobramycin does not enhance the antimicrobial activity compared to tobramycin alone, indicating there is no synergistic effect between the two entities when simply mixed. Whereas MAAPC05 showed similar activity against *S. aureus* in comparison to MAAPC01 (indicating that the terminus of conjugation did not greatly impact activity), it displayed a 2-fold increase of the MIC against *E. coli*. In contrast, MAAPC02, MAAPC03, and MAAPC04 displayed improved activity compared to MAAPC01. These results indicate the importance of the peptide transporter sequence as well as the conjugation site for tobramycin. Interestingly, MAAPC02 and MAAPC03 have nearly identical amino-acid composition as MAAPC01 (the only difference is a single glycine), but the amino acids are in a different sequence. In the MAAPC02 analog, the hydrophobic amino acids are clustered along one side of the α -helical wheel of the peptide, which confers higher amphiphilic character and greater helical propensity. In the MAAPC03 analog, the peptide has the reversed sequence of MAAPC01. There are examples in the literature that the reversed analogs of antimicrobial peptides possess equal or enhanced antimicrobial activities.^{47,48} The amphiphilicity and peptide sequence orientation might play a role on the membrane–peptide interaction. However, further experiments are required to elucidate the reasons for this improved antibacterial activity.

One of the limitations to the clinical use of AMPs as antimicrobial agents is their hemolytic activity which is associated with increased toxicity.⁴⁹ Thus, as a first assessment of the MAAPC toxicity, we investigated whether the conjugates may cause lysis of human red blood cells (hRBCs). Notably, all

MAAPCs exhibited negligible hemolytic activity against hRBCs ($HC_{50} > 500 \mu M$), which is the first indicator of the MAAPC safety toward eukaryotic cells (Table 4). Bacterial and animal cell membranes significantly differ in composition. Indeed, microbial cell surfaces contain more anionic lipids (overall negatively charged) whereas mammalian cell membranes have more lipids with neutral zwitterionic head groups (overall neutrally charged). The MAAPCs were designed to selectively discriminate between bacterial and mammalian cells. The selectivity indexes (SIs), defined as HC_{50}/MIC , for *E. coli* and *S. aureus* demonstrated great selectivity of all MAAPCs to bacteria over hRBCs (Table 5), which implies that the MAAPCs are

Table 5. Hemolytic Activity Against hRBCs and Bacterial Selectivity of MAAPCs

	HC_{50} (μM)	selectivity index (HC_{50}/MIC)	
		<i>E. coli</i> MG1655	<i>S. aureus</i> S113
MAAPC01	516.50	82.64	20.66
MAAPC02	>1000	>320	>80
MAAPC03	>1000	>320	>80
MAAPC04	>2000	>640	>160
MAAPC05	676.70	54.14	27.07

effective against bacteria without causing harm to human cells. MAAPC04 displayed the highest bacterial selectivity (SI > 640 and SI > 160 against *E. coli* and *S. aureus*, respectively) likely due to its reduced hydrophobic content.^{50,51}

Membrane Permeabilization. In order to better understand the mode of action of our conjugates, we probed the effect of the MAAPCs on the permeability of the outer (OM) and inner (IM) membranes of *E. coli*. The assays rely on the ability of a chromogenic agent to cross the membrane only when the membrane has been compromised. In the OM permeability assay, nitrocefin, a chromogenic cephalosporin is used. Nitrocefin cannot cross the OM and is excluded from the periplasmic space. If the OM is permeabilized and nitrocefin crosses, it is cleaved by a periplasmic β -lactamase inducing a color change that can be monitored with a spectrophotometer at 486 nm. In the IM permeability assay, the chromogenic substrate *ortho*-nitrophenyl- β -galactoside (ONPG) is used. Since there is no lactose permease in *E. coli* ML35 strain, ONPG cannot diffuse into the bacterial cell cytoplasm unless the IM is compromised. Upon membrane permeabilization, ONPG is cleaved by cytoplasmic β -galactosidase into *o*-

nitrophenol and galactose, inducing a color change that can be monitored spectrophotometrically at 400 nm.

While MAAPC01 induced significant permeabilization of the OM of *E. coli* D31 at a concentration lower than MICs ($2 \mu M$), the other MAAPCs displayed relatively low OM permeabilization and tobramycin had no effect (Figure 3A). At a concentration higher than MICs ($20 \mu M$), MAAPC01 and MAAPC05 demonstrated enhanced permeation activity although no significant increase was observed for MAAPC02, MAAPC03, and MAAPC04 (Figure S2). With the exception of MAAPC04, all MAAPCs disrupted, with different degrees of susceptibility, the IM of *E. coli* ML35 at a concentration of $2 \mu M$ (Figure 3B). MAAPC01 and MAAPC05 exhibited the highest permeation effect, which was comparable to the positive control (melittin). In contrast, MAAPC04 did not promote IM permeabilization. We hypothesize this occurs because of its lower hydrophobic content, which generally correlates with less lytic activity. MAAPC02 displayed unexpectedly low membrane activity, which is surprising considering that its hydrophobic and polar residues are arranged on opposite sides of the peptide assuming α -helical secondary structure. It is generally accepted that a certain level of hydrophobicity is required to penetrate the membrane of prokaryotic cells, and clustering hydrophobic amino acids in AMP structures enhances antimicrobial activity.^{50,51} However, it has also been argued that there is an optimal level of hydrophobicity above which further increase in hydrophobicity results in strong peptide self-assembly which decreases cell wall permeability.^{50,51} In general, these effects will also depend on the geometric organization and presentation of the hydrophobicity.

MAAPC01 and MAAPC05 displayed significant OM and IM permeabilization activity although these MAAPCs are less active against *E. coli* (MIC = 6.3 and $12.5 \mu M$ respectively) than the other MAAPCs (MIC = $3.1 \mu M$) that exhibit lower permeabilization and greater bactericidal activity. The inverse relationship between the activity and membrane permeabilization suggests that the ability of MAAPCs to permeabilize the *E. coli* membrane does not directly reflect their antibacterial activity on growing bacteria. This implies that the antibacterial activity of MAAPCs against actively growing bacteria is not solely dependent on bacterial membrane disruption (the mechanism of AMP bactericidal activity). Membrane permeability experiments on actively growing cells do not show other mechanisms of antibiotic entry into the cell (i.e., via active transport), and thus do not necessarily correlate with the total amount of MAAPC that enters a bacterium. However, this

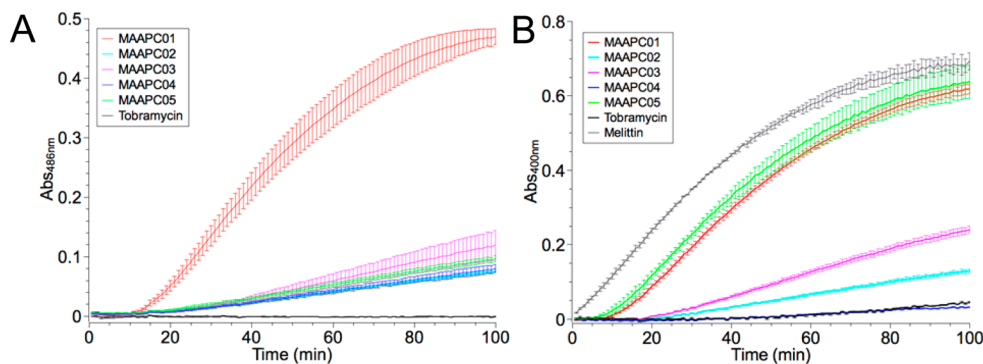


Figure 3. (A) *E. coli* D31 OM permeabilization by MAAPCs; (B) *E. coli* ML35 IM permeabilization by MAAPCs. The concentration for all tested compounds is $2 \mu M$. Data are expressed as averages \pm S.D., $n = 3$.

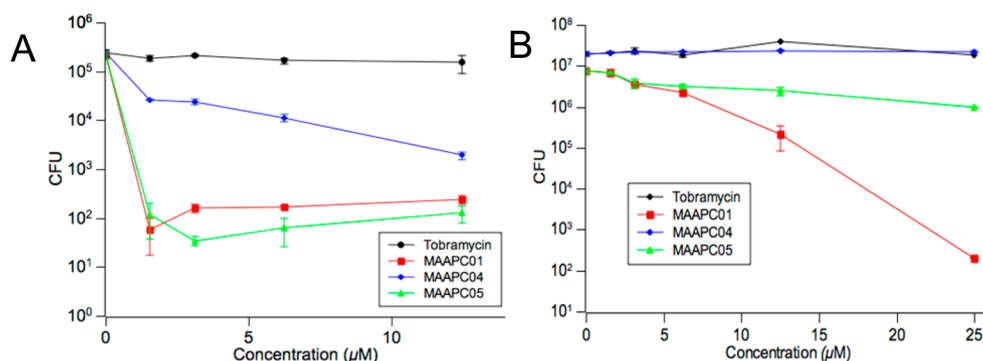


Figure 4. Killing activity of MAAPCs against persister cells: (A) *E. coli* MG1655 and (B) *S. aureus* SA113. *E. coli* MG1655 were pretreated with ciprofloxacin (1 μg/mL) while *S. aureus* SA113 were pretreated with ampicillin (100 μg/mL) for 3 h to eliminate nonpersister cells.

active drug influx is easily shut down on dormant cells (persisters), in which active transport is drastically diminished and membrane permeability is expected to more closely correlate with antibacterial activity.

Bactericidal Activity against Persister Cells. To verify the above hypothesis, we compared the bactericidal activity of MAAPC01 and MAAPC05 to the least lytic (on bacterial membrane and hRBCs), most active, and selective conjugate (MAAPC04) against persister cells with plate killing assays. *E. coli* MG1655 and *S. aureus* S113 bacteria prepared in a persistent state were incubated for 2 h with varying concentrations of MAAPCs or tobramycin (Figure 4). Consistent with previous studies,²⁴ tobramycin showed no activity against *E. coli* and *S. aureus* persistent bacteria over the entire range of tested concentrations, while MAAPC01 demonstrated remarkable dose-dependent bactericidal activity against both persistent cells. MAAPC05 had comparable killing potency to its N-terminal-conjugated analog MAAPC01 against *E. coli* persisters resulting in a 3-log reduction in colony-forming units (CFU) at a concentration of 3.1 μM lower than its MIC (12.5 μM) (Figure 4A). In contrast, MAAPC04 exhibited less than a 2-log reduction in CFU at a concentration of 12.5 μM despite it being 4-fold higher than its MIC (3.1 μM) against *E. coli*. Interestingly, MAAPC05 showed reduced activity against *S. aureus* persisters in comparison to MAAPC01 (Figure 4B). Based on the earlier observation that MAAPC05 can permeabilize the IM of *E. coli* to the same extent as MAAPC01 and the fact that *S. aureus* that are Gram-positive organisms do not possess OM, we would have anticipated similar activity for MAAPC05 and MAAPC01 against *S. aureus* persister cells. Thus, it is possible that MAAPC05 has different permeability profiles depending on whether the pathogen is Gram-positive or Gram-negative. It should be noted that MAAPC04 had no bactericidal activity against *S. aureus* persisters (Figure 4B). It is also worth noting that the antimicrobial activity observed when the unconjugated peptide was mixed with tobramycin was similar to tobramycin alone or to the peptide alone against persisters (an example for MAAPC06 against *E. coli* persisters is shown in Figure S3) indicating that the synergistic effect occurs only when the peptide and tobramycin are chemically conjugated.

Although MAAPC04 exhibits higher antimicrobial activity against actively growing bacteria, its lower antimicrobial activity against persisters correlates well with the membrane permeability assays. Furthermore, MAAPC01 and MAAPC05 exhibit both high membrane permeability and strong activity against persisters compared to their lower antimicrobial activity against

actively growing cells. These results are consistent with our hypothesis that membrane permeability is necessary to kill antibiotic-tolerant bacteria but not the primary mechanism of action in actively growing organisms.

CONCLUSION

We have synthesized a series of MAAPCs incorporating tobramycin with variations in the composition, sequence, and conjugation site of the peptide transporter. The MAAPCs exhibit good selectivity for bacterial cell membranes over mammalian cell membranes and do not induce any significant hemolysis of human red blood cells. MAAPCs exhibit better antibacterial activity against actively growing Gram-negative *E. coli* (MIC < 15 μM) than actively growing Gram-positive *S. aureus* (MIC < 25 μM). MAAPC01 exhibits the highest permeabilization of the outer membrane, with all other MAAPCs showing less permeation activity; tobramycin exhibits no outer membrane activity. MAAPC01 and MAAPC05 exhibit the highest inner membrane permeability, comparable to the control melittin. MAAPC02 and 03 exhibit less membrane activity, and MAAPC04 and tobramycin show negligible inner membrane activity. Higher levels of membrane activity correlate well with antimicrobial activity against persisters, where MAAPC01 and MAAPC05 show much better activity than tobramycin alone or MAAPC04.

Overall, we have demonstrated that we can design hybrid antibiotic peptide conjugates that can cross bacterial cell membranes that are impermeable to traditional antibiotics, and that their membrane activity and antibacterial activity can be finely tuned through small changes to the peptide transporter composition and sequence. These powerful new antibiotics show promise as novel therapies for resistant and difficult-to-treat bacterial infections.

MATERIALS AND METHODS

Materials. Reagent grade solvents such as *N,N*-dimethylformamide (DMF), ethyl acetate, dichloromethane (DCM), methanol (MeOH), and acetonitrile (CH₃CN), as well as magnesium sulfate (MgSO₄), Lysogeny broth (LB), and tris hydrochloride were purchased from Fisher Scientific. Tobramycin was purchased from TCI. Pyridine was obtained from J.T. Baker. *p*-Toluenesulfonyl chloride (TsCl), trifluoroacetic acid (TFA), thioanisole, and triisopropylsilane (TIS) were purchased from Acros Organics. Sodium azide (NaN₃) was obtained from EMD. Copper sulfate pentahydrate (CuSO₄) was purchased from Reagent World. *N*-Fmoc-L-propargylglycine (Fmoc-Pra-OH) was purchased from AAPPTEC (Louis-

ville, KY, USA). Sodium ascorbate, *N,N*-diisopropyl-*N*-ethylamine (DIEA), and triethylamine (TEA) were obtained from Alfa Aesar. 2-Chlorotriethyl chloride resin (~1 mmol/g) was obtained from ChemImpex. Hydroxybenzotriazole (HOBt) was obtained from Advanced ChemTech. 2-(1*H*-Benzotriazol-1-yl)-1,1,3,3-tetramethyluronium hexafluorophosphate (HBTU), preloaded amino acid cartridges, and melittin were purchased from AnaSpec Inc. Phenol was obtained from Amresco. Tryptic soy broth (TSB), agar, and M9 minimal salts (5X) were obtained from Difco Laboratories. Nitrocefin was purchased from BioVision. *Ortho*-nitrophenyl- β -galactoside (ONPG) and PIPES were purchased from Sigma. Human red blood cells (hRBCs) were bought from Lampire Biological Laboratories and were obtained from a single donor.

Synthesis of Tosyl-Boc₅-tobramycin (2). Boc₅-tobramycin (1) synthesized as previously described²⁴ (3.58 g, 3.70 mmol, 1 equiv) was dissolved in pyridine (85 mL) and cooled down with an ice bath. TsCl (987.5 mg, 5.18 mmol, 1.5 equiv) was added to the mixture. After stirring for 2 h at room temperature, TsCl (987.5 mg, 5.18 mmol, 1.5 equiv) was added again. The solution was stirred for 12 h at room temperature under argon. The solution was concentrated via rotary evaporation, diluted with ethyl acetate (200 mL), washed with nonsaturated brine (3 × equiv vol), dried with MgSO₄, and concentrated to dryness via rotary evaporation. The white solid was purified by silica gel chromatography to yield 1.48 g (36%). ¹H NMR (500 MHz, DMSO-*d*₆, 25 °C): δ (ppm) = 7.65–7.80 (d, 2H), 7.40–7.50 (d, 2H), 6.87 (s, 1 H, NH), 6.45–6.59 (br, 3H, NH), 6.40 (s, 1 H, NH), 4.77–5.00 (br, 5H), 4.00–4.18 (br, 3 H), 3.12–3.55 (br, 10 H), 2.39 (s, 3 H), 1.82 (m, 1 H), 1.72 (m, 1 H), 1.15–1.50 (m, 47 H). Mass analysis (MALDI-TOF): m/z 1144.545 (calcd for C₅₀H₈₃NaN₅O₂₁S [M + Na]⁺ m/z 1144.519).

Synthesis of Azido-Boc₅-tobramycin (3). Tosyl-Boc₅-tobramycin (1.48 g, 1.32 mmol, 1 equiv) was dissolved in DMF (19 mL). NaN₃ (858 mg, 13.2 mmol, 10 equiv) was added to the mixture. The solution was stirred at 80 °C for 12 h under argon. The solution was diluted with ethyl acetate (200 mL), washed with DI water (3 × equiv vol), dried with MgSO₄, and concentrated to dryness via rotary evaporation to yield 1.30 g (99%) of a white solid. ¹H NMR (300 MHz, DMSO-*d*₆, 25 °C): δ (ppm) = 6.92 (s, 1 H, NH), 6.49–6.65 (br, 3 H, NH), 6.41 (s, 1 H, NH), 4.81–5.05 (br, 5 H), 4.05 (m, 1 H), 3.65 (m, 1 H), 3.10–3.60 (br, 11 H), 1.80 (m, 2 H), 1.10–1.60 (m, 47 H). Mass analysis (MALDI-TOF): m/z 1015.551 (calcd for C₄₃H₇₆NaN₈O₁₈ [M + Na]⁺ m/z 1015.517).

Synthesis of Fmoc-Pra(BocTobra)-OH (4) by Click Reaction. Fmoc-Pra-OH (188.2 mg, 0.56 mmol, 1 equiv, AAPPTC) and azido-Boc₅-tobramycin (612.7 mg, 0.62 mmol, 1.1 equiv) were dissolved in DMF (20 mL) at 40 °C under argon. One mL of copper sulfate aqueous solution (0.28 mmol, 0.5 equiv) and 1 mL of sodium ascorbate aqueous solution (0.56 mmol, 1 equiv) were added to the mixture. The solution was stirred at 40 °C for 24 h. The solution was concentrated via rotary evaporation, diluted with ethyl acetate (200 mL), washed with water (3 × equiv vol), dried with MgSO₄, and concentrated to dryness via rotary evaporation. The white solid was purified by silica gel chromatography to yield 453 mg (61%). ¹H NMR (500 MHz, methanol-*d*₄, 25 °C): δ (ppm) = 7.80 (m, 3 H, Fmoc and triazole), 7.65 (m, 2 H, Fmoc), 7.38 (m, 2 H, Fmoc), 7.30 (m, 2 H, Fmoc), 5.08–5.15 (br, 2 H), 4.60 (m, 1 H), 4.48 (m, 2 H), 4.35 (m, 2 H), 4.22 (m, 2 H), 3.73 (t, 1 H), 3.62 (m, 3 H), 3.25–3.60 (br, 9 H), 3.20 (m, 1

H), 3.10 (m, 1 H), 2.00 (m, 2 H), 1.62 (dd, 1 H), 1.20–1.60 (br, 46 H). Mass analysis (MALDI-TOF): m/z 1350.591 (calcd for C₆₃H₉₃NaN₉O₂₂ [M + Na]⁺ m/z 1350.633).

Synthesis of MAAPC05. The (RQIKIWFQRRWPra-(Tobra)) peptide (MAAPC05) was synthesized by Fmoc/*t*-butyl batch solid-phase synthesis on an Applied Biosystems 433A automated peptide synthesizer, which allowed for direct conductivity monitoring of Fmoc deprotection. A 0.2 mmol scale synthesis was conducted using a preloaded 2-chlorotriethyl resin.

Loading of the First Amino Acid. A solution of Fmoc-Pra(BocTobra)-OH (4) (448 mg, 0.34 mmol, 1 equiv) and DIEA (235 μ L, 7.0 mmol, 4 equiv) in dry DCM (10 mL) was added to 2-chlorotriethyl chloride resin (340 mg, 0.34 mmol, 1 equiv) and the reaction stirred for 4 h. The resin was transferred into a peptide vessel fitted with a polyethylene filter disk, and washed with a solution of DCM/MeOH/DIEA (17:2:1; 3 × 20 mL), DCM (3 × 20 mL), DMF (2 × 20 mL), and DCM (2 × 20 mL). The grafting yield was determined by measuring the absorbance of *N*-(9-fluorenylmethyl)piperidine complex at 301 nm by UV–vis spectroscopy (after treatment with piperidine) and resulted 0.35 mmol/g.

Automatic Synthesis of Peptide. Subsequent Fmoc amino acids were coupled using a “conditional double coupling” protocol on a 0.2 mmol scale. The Fmoc group was cleaved from the peptide-resin using a piperidine solution and monitored by conductivity. Subsequent amino acids (5 equiv amino acid) were activated with a mixture of HBTU/HOBt/DIEA and attached to the *N*-terminal of the peptide-resin.

Cleavage of the Peptide from the Resin with Removal of the Acid-Labile Protecting Groups. This was achieved by using 10 mL of a scavenging mixture of TFA/phenol/water/thioanisole/TIS (10/0.75/0.5/0.5/0.25 v/w/v/v/v) for 3 h. The resin was filtered out with a fritted filter, rinsed with 1 mL of TFA and 20 mL of DCM, the filtrate containing the unprotected peptide was concentrated to small volume, and the product was precipitated with cold diethyl ether, isolated by filtration, and dried under vacuum overnight. The peptide was purified by preparative RP-HPLC (JASCO system) at 17 mL/min on a Waters C18 column (250 × 22 mm, 5 mm) using a gradient of A [H₂O + 0.1% TFA] and B [CH₃CN + 0.1% TFA]: 0% of B for 5 min, 0% → 70% for 7 min, 70% for 3 min, 70% → 100% for 2 min and 100% for 2 min; detection at 214 nm; *t*_r = 10.4 min. CH₃CN was evaporated under reduced pressure and the aqueous solution was freeze-dried to give a white solid (211.5 mg, 46%). Mass analysis (MALDI-TOF): m/z 2318.519 (calcd for C₁₀₄H₁₆₅N₃₆O₂₅ [M + H]⁺ m/z 2318.275).

Bacterial Strains and Media. Standard lab strains *E. coli* MG1655 and *S. aureus* SA113 are used as Gram-negative and Gram-positive strain, respectively. *E. coli* MG1655 were grown in Luria broth (LB), and SA113 were grown in Tryptic soy broth (TSB) at 37 °C. Both bacterial strains are grown under aerobic condition. Two other lab strains, *E. coli* D31 and *E. coli* ML35 are used for outer and inner membrane permeability assay, respectively.

Antibacterial Testing: MIC and MBC Determination. MICs of MAAPCs were determined in a standard microbroth dilution assay in accordance with the guidelines of the Clinical and Laboratory Standards Institute guidelines (CLSI)⁵² with suggested modifications by Hancock group.⁵³ An overnight culture of bacterial strains was diluted with the appropriate media and grown to mid log phase (OD₆₀₀ of 0.5–0.6), then

diluted 50 times before added to a 96-well microplate containing 2× serial dilutions of an MAAPC for a final count of 5×10^4 cfu/well. The plates were incubated at 37 °C for 18 h in an ambient air incubator and read for turbidity in each well. The MIC values were determined as the lowest concentration that completely inhibited bacterial growth. For the determination of MBCs, 5 μ L of bacterial suspension from each well of the MIC plate were then transferred into 100 μ L of LB or TSB in a 96-well plate and incubated for 18 h at 37 °C. The lowest concentration that revealed no visible bacterial growth after subculturing was taken as MBC. Each assay was performed in triplicate.

Hemolysis. Human red blood cells (hRBCs) (1 mL) were pelleted (3500 rpm for 5 min), washed three times with PBS buffer (PBS 10 mM plus 150 mM NaCl, pH 7.4), and resuspended in PBS buffer. The cell suspension (1 mL) was then diluted 50 times in PBS buffer (49 mL). Various concentrations of antibiotic solutions (20 μ L) were added to the diluted cell suspension (180 μ L) in a 96-well plate, and incubated with orbital shaking at 37 °C for 1 h. The cells from each well were then transferred into 1.5 mL tubes and pelleted by centrifugation (3500 rpm for 5 min). Then, 100 μ L of supernatant from each tube were collected into a clear 96-well plate, and the absorbance of the released hemoglobin was measured with a plate reader spectrophotometer at 405 nm. Hemolysis was determined relative to the negative control (PBS) and the positive control (1% v/v Triton-X-100 that lyses 100% of hRBCs). HC_{50} was defined as the antibiotic concentration causing 50% hemolysis. The hemolysis assay was performed in triplicate.

Outer Membrane Permeability Assay on *E. coli* D31. The method similar to previous studies⁵⁴ is used. Briefly, *E. coli* D31 were aerobically cultured in LB supplemented with 100 μ g/mL ampicillin. An overnight culture of bacterial suspension was regrown to mid log phase (OD_{600} of 0.5–0.6), then washed and resuspended in 10 mM PBS buffer supplemented with 100 mM NaCl at pH 7.4. The washed cells were then diluted 1:5 in fresh PBS buffer containing nitrocefin (55 μ g/mL), and 135 μ L of the diluted cells were added to each well of a 96-well plate. Just prior to reading, 15 μ L of various concentrations of antibiotic solutions were added to the wells. The kinetics of nitrocefin cleavage were measured for 100 min at 37 °C by determining the absorbance at 486 nm using a plate reader spectrophotometer. All assays were performed in triplicate.

Inner Membrane Permeability Assay on *E. coli* ML35. The method similar to previous studies^{24,55} is used. *E. coli* ML35 were aerobically cultured in TSB. An overnight culture of *E. coli* ML35 was diluted and grown to mid log phase (OD_{600} of 0.5–0.6), then washed and resuspended in 10 mM Tris buffer supplemented with 1% v/v TSB at pH 7.4 (Tris-TSB). The washed cells were then diluted 1:3 in fresh Tris-TSB buffer containing 2.8 mM ONPG, and 135 μ L of the diluted cells was added to each well of a 96-well plate. Just prior to reading, 15 μ L of antibiotic solutions was added to the wells to a final concentration of 2 μ M. Melittin was used as a positive control. The kinetics of ONPG hydrolysis were measured for 100 min at 37 °C by determining the absorbance at 400 nm using a plate reader spectrophotometer. All assays were performed in triplicate.

Persister Cell Assays. The procedure for preparing *E. coli* MG1655 and *S. aureus* S113 persister cells is based on previous protocols.²⁴

E. coli cells were grown in LB for 18 h at 37 °C to obtain stationary phase cultures. Nonpersister cells were eliminated by adding ciprofloxacin to a final concentration of 1 μ g/mL, followed by a 3 h incubation at 37 °C. *E. coli* cells were pelleted (5000 rpm for 5 min), washed in M9 minimal media, and resuspended in M9 minimal media to a final bacteria suspension of 5×10^6 CFU/mL. 10 μ L *E. coli* suspension was added into 90 μ L of M9 media containing various concentrations of antibiotics in 96-well plates for a final cell count of 5×10^5 CFU/well. The plates were sealed and incubated with shaking at 37 °C incubator for 2 h. After incubation, the assay mixture is serially diluted with M9 media and plated on LB agar. The agar plates were incubated overnight at 37 °C to yield visible colonies. The *E. coli* persister assays were performed in duplicate.

S. aureus cells were grown in TSB for 18 h at 37 °C to obtain stationary phase cultures. Nonpersister cells were eliminated by adding ampicillin to a final concentration of 100 μ g/mL, followed by a 3 h incubation at 37 °C. *S. aureus* cells were pelleted (5000 rpm for 5 min), washed with 10 mM PIPES buffer (pH 7.4), and resuspended in PIPES buffer to a final bacteria stock solution of 1×10^8 CFU/mL. 10 μ L *S. aureus* suspension was added into 90 μ L of PIPES buffer containing various concentrations of antibiotics in 96-well plates for a final cell count of 1×10^7 CFU/well. The plates were sealed and incubated with shaking at 37 °C incubator for 2 h. After incubation, the assay mixture was 10× serially diluted with PIPES buffer and plated on LB agar plates. The agar plates were incubated overnight at 37 °C to yield visible colonies. The *S. aureus* persister assays were performed in duplicate.

■ ASSOCIATED CONTENT

📄 Supporting Information

The Supporting Information is available free of charge on the ACS Publications website at DOI: 10.1021/acs.bioconjchem.6b00725.

Chemical structures of MAAPC01-05; *E. coli* D31 OM permeabilization by MAAPCs; killing activity of MAAPC04 (PDF)

■ AUTHOR INFORMATION

Corresponding Authors

*E-mail: gclwong@seas.ucla.edu. Fax: (+1) 310-794-5956.

*E-mail: akasko@ucla.edu. Fax: (+1) 310-794-6341.

ORCID

Andrea M. Kasko: 0000-0003-2355-6258

Notes

The authors declare the following competing financial interest(s): A.M.K., G.C.L.W., S.D., N.S. and W.X. are co-inventors of intellectual property described in this report.

■ ACKNOWLEDGMENTS

This work is supported by NSF grant DMR-1411329.

■ ABBREVIATIONS

Boc, *tert*-butyloxycarbonyl; Boc₂O, di(*tert*butyl)dicarbonate; Fmoc, 9-fluorenylmethoxycarbonyl; MALDI-TOF, matrix assisted laser desorption ionization time-of-flight; NMR, nuclear magnetic resonance; RP-HPLC, reversed-phase high performance liquid chromatography

REFERENCES

- (1) Avent, M. L., Rogers, B. A., Cheng, A. C., and Paterson, D. L. (2011) Current Use of Aminoglycosides: Indications, Pharmacokinetics and Monitoring for Toxicity. *Intern. Med. J.* 41, 441–449.
- (2) Poehlsgaard, J., and Douthwaite, S. (2005) The Bacterial Ribosome as a Target for Antibiotics. *Nat. Rev. Microbiol.* 3, 870–881.
- (3) Magnet, S., and Blanchard, J. S. (2005) Molecular Insights into Aminoglycoside Action and Resistance. *Chem. Rev. (Washington, DC, U. S.)* 105, 477–498.
- (4) Fourmy, D., Recht, M. I., Blanchard, S. C., and Puglisi, J. D. (1996) Structure of the a Site of *Escherichia Coli* 16s Ribosomal Rna Complexed with an Aminoglycoside Antibiotic. *Science* 274, 1367.
- (5) Chow, J. W. (2000) Aminoglycoside Resistance in Enterococci. *Clin. Infect. Dis.* 31, 586–589.
- (6) Mingeot-Leclercq, M.-P., Glupczynski, Y., and Tulkens, P. M. (1999) Aminoglycosides: Activity and Resistance. *Antimicrob. Agents Chemother.* 43, 727–737.
- (7) Allen, N. E., Alborn, W. E., Hobbs, J. N., and Kirst, H. A. (1982) 7-Hydroxytropolone: An Inhibitor of Aminoglycoside-2"-O-Adenylyltransferase. *Antimicrob. Agents Chemother.* 22, 824–831.
- (8) Daigle, D. M., McKay, G. A., and Wright, G. D. (1997) Inhibition of Aminoglycoside Antibiotic Resistance Enzymes by Protein Kinase Inhibitors. *J. Biol. Chem.* 272, 24755–24758.
- (9) Boehr, D. D., Draker, K.-a., Koteva, K., Bains, M., Hancock, R. E., and Wright, G. D. (2003) Broad-Spectrum Peptide Inhibitors of Aminoglycoside Antibiotic Resistance Enzymes. *Chem. Biol.* 10, 189–196.
- (10) Li, J., Wang, J., Czyryca, P. G., Chang, H., Orsak, T. W., Evanson, R., and Chang, C.-W. T. (2004) Application of Glycodiversification: Expedient Synthesis and Antibacterial Evaluation of a Library of Kanamycin B Analogues. *Org. Lett.* 6, 1381–1384.
- (11) Bastida, A., Hidalgo, A., Chiara, J. L., Torrado, M., Corzana, F., Pérez-Cañadillas, J. M., Groves, P., Garcia-Junceda, E., Gonzalez, C., Jimenez-Barbero, J., et al. (2006) Exploring the Use of Conformationally Locked Aminoglycosides as a New Strategy to Overcome Bacterial Resistance. *J. Am. Chem. Soc.* 128, 100–116.
- (12) Fridman, M., Belakhov, V., Yaron, S., and Baasov, T. (2003) A New Class of Branched Aminoglycosides: Pseudo-Pentasaccharide Derivatives of Neomycin B. *Org. Lett.* 5, 3575–3578.
- (13) Hanessian, S., Tremblay, M., and Swayze, E. E. (2003) Tobramycin Analogues with C-5 Aminoalkyl Ether Chains Intended to Mimic Rings Iii and Iv of Paromomycin. *Tetrahedron* 59, 983–993.
- (14) Aggen, J. B., Armstrong, E. S., Goldblum, A. A., Dozzo, P., Linsell, M. S., Gliedt, M. J., Hildebrandt, D. J., Feeney, L. A., Kubo, A., Matias, R. D., et al. (2010) Synthesis and Spectrum of the Neoglycoside Achn-490. *Antimicrob. Agents Chemother.* 54, 4636–4642.
- (15) Zhanel, G. G., Lawson, C. D., Zelenitsky, S., Findlay, B., Schweizer, F., Adam, H., Walkty, A., Rubinstein, E., Gin, A. S., Hoban, D. J., et al. (2012) Comparison of the Next-Generation Aminoglycoside Plazomicin to Gentamicin, Tobramycin and Amikacin. *Expert Rev. Anti-Infect. Ther.* 10, 459–473.
- (16) Sun, J., Deng, Z., and Yan, A. (2014) Bacterial Multidrug Efflux Pumps: Mechanisms, Physiology and Pharmacological Exploitations. *Biochem. Biophys. Res. Commun.* 453, 254–267.
- (17) Pu, Y., Zhao, Z., Li, Y., Zou, J., Ma, Q., Zhao, Y., Ke, Y., Zhu, Y., Chen, H., Baker, Matthew, A. B., et al. (2016) Enhanced Efflux Activity Facilitates Drug Tolerance in Dormant Bacterial Cells. *Mol. Cell* 62, 284–294.
- (18) Delcour, A. H. (2009) Outer Membrane Permeability and Antibiotic Resistance. *Biochim. Biophys. Acta, Proteins Proteomics* 1794, 808–816.
- (19) Nikaido, H. (1988) Bacterial Resistance to Antibiotics as a Function of Outer Membrane Permeability. *J. Antimicrob. Chemother.* 22, 17–22.
- (20) Allison, K. R., Brynildsen, M. P., and Collins, J. J. (2011) Metabolite-Enabled Eradication of Bacterial Persisters by Aminoglycosides. *Nature* 473, 216–220.
- (21) Taber, H. W., Mueller, J., Miller, P., and Arrow, A. (1987) Bacterial Uptake of Aminoglycoside Antibiotics. *Microbiol. Rev.* 51, 439.
- (22) Davis, B. D. (1987) Mechanism of Bactericidal Action of Aminoglycosides. *Microbiol. Rev.* 51, 341.
- (23) Cohen, N. R., Lobritz, M. A., and Collins, J. J. (2013) Microbial Persistence and the Road to Drug Resistance. *Cell Host Microbe* 13, 632–642.
- (24) Schmidt, N. W., Deshayes, S., Hawker, S., Blacker, A., Kasko, A. M., and Wong, G. C. L. (2014) Engineering Persister-Specific Antibiotics with Synergistic Antimicrobial Functions. *ACS Nano* 8, 8786–8793.
- (25) Zasloff, M. (2002) Antimicrobial Peptides of Multicellular Organisms. *Nature* 415, 389–395.
- (26) Brogden, K. A. (2005) Antimicrobial Peptides: Pore Formers or Metabolic Inhibitors in Bacteria? *Nat. Rev. Microbiol.* 3, 238–250.
- (27) Hancock, R. E. W., and Sahl, H.-G. (2006) Antimicrobial and Host-Defense Peptides as New Anti-Infective Therapeutic Strategies. *Nat. Biotechnol.* 24, 1551–1557.
- (28) Schmidt, N. W., and Wong, G. C. (2013) Antimicrobial Peptides and Induced Membrane Curvature: Geometry, Coordination Chemistry, and Molecular Engineering. *Curr. Opin. Solid State Mater. Sci.* 17, 151–163.
- (29) Mishra, A., Lai, G. H., Schmidt, N. W., Sun, V. Z., Rodriguez, A. R., Tong, R., Tang, L., Cheng, J., Deming, T. J., Kamei, D. T., et al. (2011) Translocation of Hiv Tat Peptide and Analogues Induced by Multiplexed Membrane and Cytoskeletal Interactions. *Proc. Natl. Acad. Sci. U. S. A.* 108, 16883–16888.
- (30) Schmidt, N. W., Mishra, A., Wang, J., DeGrado, W. F., and Wong, G. C. L. (2013) Influenza Virus a M2 Protein Generates Negative Gaussian Membrane Curvature Necessary for Budding and Scission. *J. Am. Chem. Soc.* 135, 13710–13719.
- (31) Sahl, H.-G., Pag, U., Bonness, S., Wagner, S., Antcheva, N., and Tossi, A. (2005) Mammalian Defensins: Structures and Mechanism of Antibiotic Activity. *J. Leukocyte Biol.* 77, 466–475.
- (32) Schmidt, N. W., Agak, G. W., Deshayes, S., Yu, Y., Blacker, A., Champer, J., Xian, W., Kasko, A. M., Kim, J., and Wong, G. C. L. (2015) Pentobra: A Potent Antibiotic with Multiple Layers of Selective Antimicrobial Mechanisms against *Propionibacterium Acnes*. *J. Invest. Dermatol.* 135, 1581–1589.
- (33) Schmidt, N. W., Lis, M., Zhao, K., Lai, G. H., Alexandrova, A. N., Tew, G. N., and Wong, G. C. L. (2012) Molecular Basis for Nanoscopic Membrane Curvature Generation from Quantum Mechanical Models and Synthetic Transporter Sequences. *J. Am. Chem. Soc.* 134, 19207–19216.
- (34) Schmidt, N., Mishra, A., Lai, G. H., and Wong, G. C. L. (2010) Arginine-Rich Cell-Penetrating Peptides. *FEBS Lett.* 584, 1806–1813.
- (35) Schmidt, N. W., Mishra, A., Lai, G. H., Davis, M., Sanders, L. K., Tran, D., Garcia, A., Tai, K. P., McCray, P. B., Ouellette, A. J., et al. (2011) Criterion for Amino Acid Composition of Defensins and Antimicrobial Peptides Based on Geometry of Membrane Destabilization. *J. Am. Chem. Soc.* 133, 6720–6727.
- (36) Hu, K., Schmidt, N. W., Zhu, R., Jiang, Y., Lai, G. H., Wei, G., Palermo, E. F., Kuroda, K., Wong, G. C. L., and Yang, L. (2013) A Critical Evaluation of Random Copolymer Mimesis of Homogeneous Antimicrobial Peptides. *Macromolecules* 46, 1908–1915.
- (37) Lee, E. Y., Fulan, B. M., Wong, G. C. L., and Ferguson, A. L. (2016) Mapping Membrane Activity in Undiscovered Peptide Sequence Space Using Machine Learning. *Proc. Natl. Acad. Sci. U. S. A.* 113, 13588–13593.
- (38) Döring, G., Flume, P., Heijerman, H., and Elborn, J. S. (2012) Treatment of Lung Infection in Patients with Cystic Fibrosis: Current and Future Strategies. *J. Cystic Fibrosis* 11, 461–479.
- (39) Asensio, J. L., Hidalgo, A., Bastida, A., Torrado, M., Corzana, F., Chiara, J. L., Garcia-Junceda, E., Canada, J., and Jimenez-Barbero, J. (2005) A Simple Structural-Based Approach to Prevent Aminoglycoside Inactivation by Bacterial Defense Proteins. Conformational Restriction Provides Effective Protection against Neomycin-B Nucleotidylation by Ant4. *J. Am. Chem. Soc.* 127, 8278–8279.

- (40) Hanessian, S., Masse, R., and Capmeau, M.-L. (1977) Aminoglycoside Antibiotics: Synthesis of 5"-Amino-5"-Deoxyneomycin and 5"-Amino-5"-Deoxyparomomycin. *J. Antibiot.* 30, 893–896.
- (41) Bera, S., Zhanel, G. G., and Schweizer, F. (2008) Design, Synthesis, and Antibacterial Activities of Neomycin-Lipid Conjugates: Polycationic Lipids with Potent Gram-Positive Activity. *J. Med. Chem.* 51, 6160–6164.
- (42) Giangaspero, A., Sandri, L., and Tossi, A. (2001) Amphipathic A Helical Antimicrobial Peptides. *Eur. J. Biochem.* 268, 5589–5600.
- (43) Eisenberg, D., Weiss, R. M., Terwilliger, T. C., and Wilcox, W. (1982) Hydrophobic Moments and Protein Structure. *Faraday Symp. Chem. Soc.* 17, 109–120.
- (44) Kyte, J., and Doolittle, R. F. (1982) A Simple Method for Displaying the Hydrophobic Character of a Protein. *J. Mol. Biol.* 157, 105–132.
- (45) Hessa, T., Kim, H., Bihlmaier, K., Lundin, C., Boekel, J., Andersson, H., Nilsson, I., White, S. H., and von Heijne, G. (2005) Recognition of Transmembrane Helices by the Endoplasmic Reticulum Translocon. *Nature* 433, 377–381.
- (46) Gonzalez, L., and Spencer, J. (1998) Aminoglycosides: A Practical Review. *American Family Physician* 58, 1811–20.
- (47) Juretić, D., Chen, H.-C., Brown, J. H., Morell, J. L., Hendler, R. W., and Westerhoff, H. V. (1989) Magainin 2 Amide and Analogues Antimicrobial Activity, Membrane Depolarization and Susceptibility to Proteolysis. *FEBS Lett.* 249, 219–223.
- (48) Wei, S.-Y., Wu, J.-M., Kuo, Y.-Y., Chen, H.-L., Yip, B.-S., Tzeng, S.-R., and Cheng, J.-W. (2006) Solution Structure of a Novel Tryptophan-Rich Peptide with Bidirectional Antimicrobial Activity. *J. Bacteriol.* 188, 328–334.
- (49) Chen, Y., Mant, C. T., Farmer, S. W., Hancock, R. E. W., Vasil, M. L., and Hodges, R. S. (2005) Rational Design of A-Helical Antimicrobial Peptides with Enhanced Activities and Specificity/Therapeutic Index. *J. Biol. Chem.* 280, 12316–12329.
- (50) Jiang, Z., Vasil, A. I., Vasil, M. L., and Hodges, R. S. (2014) Specificity Determinants Improve Therapeutic Indices of Two Antimicrobial Peptides Piscidin 1 and Dermaseptin S4 against the Gram-Negative Pathogens *Acinetobacter Baumannii* and *Pseudomonas Aeruginosa*. *Pharmaceuticals* 7, 366–391.
- (51) Kuroda, K., Caputo, G. A., and DeGrado, W. F. (2009) The Role of Hydrophobicity in the Antimicrobial and Hemolytic Activities of Polymethacrylate Derivatives. *Chem. - Eur. J.* 15, 1123–1133.
- (52) Clinical and Laboratory Standards Institute, Methods for Dilution Antimicrobial Susceptibility Tests for Bacteria That Grow Aerobically, 10th ed.; Approved Standard M07-A10.; Wayne, PA, USA, 2015.
- (53) Wiegand, I., Hilpert, K., and Hancock, R. E. (2008) Agar and Broth Dilution Methods to Determine the Minimal Inhibitory Concentration (Mic) of Antimicrobial Substances. *Nat. Protoc.* 3, 163–175.
- (54) Sovadinova, I., Palermo, E. F., Urban, M., Mpija, P., Caputo, G. A., and Kuroda, K. (2011) Activity and Mechanism of Antimicrobial Peptide-Mimetic Amphiphilic Polymethacrylate Derivatives. *Polymers* 3, 1512–1532.
- (55) Llenado, R. A., Weeks, C. S., Cocco, M. J., and Ouellette, A. J. (2009) Electropositive Charge in A-Defensin Bactericidal Activity: Functional Effects of Lys-for-Arg Substitutions Vary with the Peptide Primary Structure. *Infect. Immun.* 77, 5035–5043.